STATUS OF THE CRYSTALLOGRAPHY BEAMLINES AT PETRA III

Anja Burkhardt, Tim Pakendorf, Bernd Reime, Jan Meyer, Pontus Fischer, Nicolas Stübe, Saravanan Panneerselvam, Olga Lorbeer, Karolina Stachnik, Martin Warmer, Philip Rödig, Dennis Göries, and Alke Meents*

Deutsches Elektronen-Synchrotron DESY, Photon Science, Notkestrasse 85, 22607 Hamburg, Germany

*e-mail: alke.meents@desy.de

Abstract

Since 2013, three beamlines for macromolecular crystallography are available to users at the third-generation synchrotron PETRA III in Hamburg: P11, P13 and P14, the latter two operated by EMBL. Beamline P11 is operated by DESY and is equipped with a Pilatus 6M detector. Together with the photon flux of 2×10^{13} ph/s provided by the very brilliant X-ray source of PETRA III, a full data set can be typically collected in less than 2 min. P11 provides state-of-the-art microfocusing capabilities with beam sizes down to 1×1 µm^2, which makes the beamline ideally suited for investigation of microcrystals and serial crystallography experiments. An automatic sample changer allows fast sample exchange in less than 20 s, which enables high-throughput crystallography and fast crystal screening. For sample preparation, an S2 biosafety laboratory is available in close proximity to the beamline.

1. Introduction

1.1. Facility Information

The large scale research facility DESY (Deutsches Elektronen-Synchrotron) is located in Hamburg, Germany, and is a member of the Helmholtz Association. DESY provides access to two facilities, the free-electron laser FLASH and the PETRA III synchrotron.
FLASH comprises two FEL (free-electron laser) undulator lines in separate tunnels which can be operated in parallel. FLASH I started user operation in summer 2005 as the first FEL for VUV and soft X-ray energies. First lasing at FLASH II was achieved in summer 2014.
PETRA III is one of the most brilliant storage-ring-based X-ray sources in the world. The third-generation 6 GeV synchrotron operates in top-up mode at a beam current of 100 mA. PETRA III provides a very low emittance of only 1 nmrad, which allows a large amount of photons to be focused into a very small spot of a few square micrometers [1, 2]. For macromolecular X-ray crystallography (MX) this has great potential, especially for structural investigations of microcrystals and large molecular complexes. The PETRA III experimental hall runs along one octant of the PETRA storage ring and provides currently space for 14 beamlines. In spring 2014, the PETRA extension project was started. Within this project, 10 new beamlines allocated to two new experimental halls are currently under construction. The first two PETRA extension beamlines will be dedicated to X-ray absorption spectroscopy and will start commissioning in autumn 2015.

1.2. Proposal System at PETRA III

Beamtime for users at PETRA III is available 24 h per day, six days a week (Monday, Tuesday, and Thursday to Sunday). For DESY-operated beamlines proposals can be submitted via the online portal DOOR (DESY Online Office for Research with Photons) [3]. Users can apply for beamtime twice a year. The deadlines for proposal submission are typically in March (for the second half of the current year) and September (for the first half of the ensuing year). There are two types of proposals: 1) Regular proposals, which are valid for six months and one beamtime only; 2) Long-Term Projects (LTP), which are valid for two years and for a total of four consecutive beamtime applications at one beamline. LTPs are available to external user groups who wish to contribute substantially to the development of the beamline. More details on the DESY proposal system can be found on the DESY Photon Science webpage [4].
At P11 priority access is granted for beamline funding partners, the Max Planck Society, the Helmholtz Association (research field 'Health'), and the University of Luebeck. In addition, all MX beamlines at PETRA III provide transnational access via BioStruct-X [5]. Within the framework of this project, European users can be reimbursed for travel and accommodation during their experiment. BioStruct-X proposals can be submitted as Block Allocation Group (BAG) and as Single Project (SP).

2. Crystallography Beamlines at PETRA III

2.1.Overview

Three out of the 14 beamlines at PETRA III are dedicated to macromolecular crystallography (see Figure 1): P11, which is operated by DESY [6], and the two EMBL beamlines P13 [7] and P14 [8]. In the future, a beamline for chemical crystallography (P24) is planned within the framework of the PETRA extension project. The characteristics of the three MX beamlines at PETRA III are summarized in Table 1.

2.2. Beamline P11 @ DESY

DESY beamline P11 provides two state-of-the-art endstations for structural investigations of biological samples at different length scales: an X-ray microscope with a resolution of up to 10 nm [9, 10, 11] and a crystallography experiment. The crystallography endstation (shown in Figure 2) is operated between 5.5 keV and 30 keV and provides full SAD/MAD capability. The X-ray beam size at the experiment can be freely chosen between 4 × 9 µm² and 300 × 300 µm² (v × h) using the full flux from the source (2×10^{13} ph/s at 12 keV). Smaller beam sizes down to 1 × 1 µm² can be realized at the cost of flux with 2×10^{11} ph/s (see Figure 3). This makes P11 ideally suited for structural investigations of microcrystals and serial crystallography experiments. In addition, P11 is equipped with a fast automatic sample changer and a large capacity storage Dewar which offers excellent conditions for high-throughput crystallography and fast crystal screening. A more detailed description of the P11 crystallography endstation is given in section 3.

2.3. Macromolecular Crystallography Beamlines P13 and P14 (MX1 and MX2) @ EMBL

EMBL beamlines P13 and P14 are fully dedicated to biological macromolecular X-ray crystallography. P13 is operated at energies between 4.5 keV and 17.5 keV. At 5 keV, the total photon flux is higher than 5×10^{11} ph/s which allows for optimized SAD/MAD data collection. The beam size can be adjusted between 20 × 30 μm^2 (v × h) and 70 × 150 μm^2 (v × h) at the sample position. The beamline is

equipped with an MD2 instrument (Arinax, Morains, France) including a mini-kappa goniostat and a helium cone. The MARVIN sample changing robot allows automatic sample exchange in less than 1 min [7].
At P14 the energy range is freely tunable between 6 keV and 20 keV. The beamline provides microbeam capability. The minimum beam size can be adjusted to 5×5 µm^2 (v × h) with 5×10^{12} ph/s in the focal spot. The MD3 diffractometer (Arinax, Morains, France) in place is mounted with its spindle axis in vertical configuration, which allows data collection from frozen samples as well as plate screening at room temperature [8].

3. The Bio-imaging and Diffraction Beamline P11

P11 is in user operation since January 2013. Basis of beamline design was to make full use of the excellent source properties of PETRA III, to deliver most of the photons from the source into a very small focal spot at the sample position, and to provide a very stable instrument to the user community.

3.1. Optics Concept

The optics concept of the beamline is shown in Figure 4. P11 is supplied with photons from a 2 m U32 undulator (minimum gap: 9.5 mm; period length: 31.4 mm) located in a high-β section of the PETRA III storage ring. Monochromatization of the X-ray beam is achieved by an LN_2 cooled double crystal monochromator (FMB Oxford Ltd., Oxford, United Kingdom) located at 36.65 m downstream from the source. The monochromator is followed by two horizontally deflecting KB (Kirkpatrick-Baez) mirrors at 38.90 m and 39.80 m and a vertically deflecting KB mirror at 40.93 m. Two horizontal mirrors, both deflecting in the same direction, are required to achieve beam separation ($2 \times 5 = 10$ mrad) from the neighboring beamline P12, which is using the same straight section with a canted undulator at a canting angle of 5 mrad. The KB mirrors are manufactured from silicon and are coated with Pd and Pt to provide X-ray energies of up to 30 keV to the experiment. Switching between coated and uncoated layers takes less than 2 min. For standard crystallography experiments grazing angles are adjusted to 2.5 mrad for each of the three KB mirrors ('three mirror configuration'). In order to efficiently suppress higher harmonics at energies below 8 keV the beamline can be operated in a ‘two mirror configuration'. In this mode, one horizontal mirror is retracted from the beam path and the grazing angle of the other horizontal mirror is set to 5 mrad. The grazing angle of the vertical mirror is left unchanged at 2.5 mrad. Using this approach, the beam position in the experimental hutch is kept at the same position for both operation modes. All KB mirrors can be dynamically bent and, in the case of crystallography experiments, are used to generate a secondary source at 65.50 m with a size of 25×210 µm^2 (FWHM, v × h).
A second refocusing KB system (see Figure 5A) consisting of a vertically and a horizontally deflecting KB mirror is located in the experimental hutch at 72.77 m and 72.95 m from the source (7.27 m and 7.45 m from the secondary source). Dynamical bending of the secondary KB mirrors allows refocusing of the X-ray beam, thereby accepting the full flux from the source (2×10^{13} ph/s at 12 keV). The slope errors of the unmounted mirror substrates were measured to be 0.72 µrad (rms) for the vertical mirror and 1.45 µrad (rms) for the horizontal mirror using a long trace profiler. The slope error for the horizontal mirror clamped onto the mechanical mirror bender was measured to be 1.64 µrad (rms) under focusing conditions. This shows that very little deformation is induced due to the mirror clamping. With refocusing using the second KB system beam sizes between 4×9 µm^2 (2nd KB system fully bent) and 300×300 µm^2 (2nd KB system flat, FWHM, v × h) can be generated at the sample position at 73.30 m. Smaller beam sizes down to 1×1 µm² with more than 2×10^{11} ph/s can be achieved by slitting down the secondary source aperture at the cost of flux, and can be routinely

realized in less than a minute. With fine-tuning of the X-ray optics accompanied by knife edge scans the secondary source aperture size can be increased and a photon flux of more than 6×10^{11} ph/s in a 1 × 1 µm^2 can be achieved. Switching between different beam foci by dynamical bending is typically realized in less than 30 s, and is currently performed manually. An automatization of this procedure is under development and its implementation into the beamline control software is planned for spring 2016, together with a fully automated energy change. The two P11 KB mirror systems are in-house developments and are now commercially available from the DESY spin-off company suna-precision, Germany [12].

3.2. Feedback System

P11 provides a very stable setup ideally suited for micro- and nanobeam applications. Key element of the experimental hutch is an 8-meter-long granite support which carries the two experimental endstations. Vibration amplitudes measured on top of the granite were less than 20 nm. The beam position is stabilized using a closed loop feedback system. For this, two independent X-ray beam position monitors (XBPM's), being located 2 m behind the monochromator and at the position of the secondary source, are permanently installed in the beam path. Both XBPM's are based on 10 µm thick CVD diamond foils equipped with quadrant electrodes. Horizontal beam position control is based on adjustment of the grazing angle of the second horizontal KB mirror at 39.80 m. Vertical beam corrections are based on changing the pitch of the second monochromator crystal. In theory it would also be possible to change the grazing angle of the vertical deflecting mirror for beam position control but it turned out a better flux stability with relative intensity variations well below 0.5% is achieved by adjusting the pitch of the second monochromator crystal. This approach is in particular advantageous after events causing changes to the thermal load on the first crystal. By adjusting the pitch of the second crystal it is guaranteed that small heat induced changes of the d-spacing of the first crystal, which translate into a slightly different energy, are compensated by small changes of the diffraction angle of the second crystal. The small wavelength changes resulting from this approach are negligible. The feedback system which is typically operated at 1 Hz provides a long term beam stability of better than 1 µm and is an in-house development of beamline P11.

3.3. Diffractometer

The in-house developed high-precision single axis goniostat at P11 is equipped with a compact air-bearing spindle in a horizontal configuration (see Figure 5B) and is commercially available from suna-precision, Germany. A piezo-motor driven crystal centering stage allows sample positioning with 10 nm accuracy and 50 nm repeatability. The P11 goniostat has a combined SOC (sphere of confusion) of less than 100 nm and a wobble of less than 1 µrad. This matches the requirements for measurements of microcrystals with micrometer-sized X-ray beams. For visual crystal detection, an on-axis microscope with an optical resolution of 2 µm is installed. In addition, apertures, a collimator, a flux diode and a scintillator screen are located on piezo-driven positioning elements, which are mounted on a flexible rail system. They can be individually driven into the X-ray beam for background reduction and beam diagnostics.

3.4. High-throughput Crystallography

The P11 crystallography endstation is equipped with a Pilatus 6M-F detector (Dectris Ltd., Baden, Switzerland), which allows for fast shutter-less operation with frame rates of up to 25 Hz. Thereby a full set of oscillation data can be collected in less than 120 s. In addition, a sample changing robot enables fully automated rapid sample exchange in less than 20 s (see Figure 5C). The P11 sample

changer consists of a Stäubli robotic arm (Stäubli Tec-Systems GmbH, Bayreuth, Germany) that is equipped with an in-house-designed gripper. The flexure-based, cryogenic sample gripper has been commercialized by suna-precision, Germany. A large storage Dewar, based on the uni-puck standard, provides capacity for 368 samples. This makes beamline P11 also well-suited for high-throughput crystallography experiments and for screening a large number of samples in short time.

3.5. Sample Preparation

A laboratory which is classified as biosafety level 2 is located in the vicinity of the beamline. The BioLab is equipped for standard protein crystallization and cell culture experiments. In addition, a Leica 205C stereo microscope including a micromanipulator for mounting of microcrystals and a Nikon Ti inversed fluorescence microscope are available to the users.

3.6. Computational Infrastructure

During their beamtime, P11 users have access to a 40-core workgroup server for fast data processing using XDS [13] or MOSFLM [14]. For structure solution and refinement all relevant software packages, such as SHELX [15], Phenix [16], CCP4 [17], COOT [18], and Olex2 [19], are installed on the workgroup server.
Experiment control at P11 is carried out using an in-house-developed Python-based Graphical User Interface (GUI). In addition to standard data collection, the GUI provides several features for micro-crystallography - such as an interface for serial crystallography and a grid scanning option. Grid scans can be performed with and without ϕ rotation at each position. This allows fully automated data collection from hundreds to thousands of microcrystals, which can be carried on *e.g.* standard micro-meshes or micro-chips [20]. DESY is a member of the MXCuBE consortium which is a collaboration between seven European light sources and Global Phasing Ltd.. The implementation of MXCuBE version 3 as a new Graphical User Interface is intended in the near future. In addition, remote experiment control is planned.

4. Research Highlights

4.1. Data Collection on Large Molecular Complexes

The flexible X-ray optics at P11 allow for tailoring the beam properties to the experimental requirements. By focusing the beam on the detector, a large parallel beam can be generated for the investigation of large unit cell systems - such as large molecular complexes, membrane proteins or virus crystals. Using the 'parallel beam option', the structure of a large unit cell system which contains a 1300-Å-long cell-axis could be solved (see Figure 6). In the diffraction pattern (see Figure 6, left, inset) clearly separated Bragg reflections can be observed. Moreover, the structure of the light-harvesting membrane protein photosystem II could be refined in its native-like arrangement to 2.44 Å resolution [21].

4.2. Serial Crystallography

Microcrystals are very sensitive towards ionizing X-ray radiation and only a few images can be collected per microcrystal before significant signs of radiation damage are observed. Complete data sets are therefore usually assembled from a large number of individual diffraction patterns acquired from many different single crystals. Such so-called serial crystallography experiments have been

successfully performed at beamline P11 at PETRA III.
For room temperature experiments a suspension of microcrystals continuously flows across the X-ray beam [22]. In a proof-of-principle demonstration, the structure of hen egg-white lysozyme could be refined to 2.1 Å resolution. The final electron density map was calculated from 40233 single-crystal indexed diffraction patterns. In recent serial crystallography experiments at P11, crystals were delivered in a LCP (lipidic cubic phase) jet and by a tape drive to the X-ray beam.
For cryogenic data collection, up to thousands of microcrystals can be mounted on a micro-fabricated sample holder from single crystalline silicon which contains micrometer-sized pores. Ideally, every micropore carries a single microcrystal. The mother liquor surrounding the microcrystals can be removed by blotting using a filter paper. This allows an almost background-free data collection with a significantly improved signal-to-noise ratio. Serial crystallography experiments on such silicon chips have been successfully performed on microcrystals at 100 K, as described in [20]. It is planned to implement our microchip-based serial crystallography method into the P11 beamline infrastructure and make it available as a standard experiment to our beamline users. For this purpose, a flexure-based X,Y-scanning unit which allows for sample positioning with a repeatability of ±12 nm (peak-to-peak), and an in-house-designed plunge-freezing device with automated blotting and subsequent chip-freezing are available at the beamline (see Figure 7). In addition, a software tool for automatic chip scanning (with and without ϕ rotation at each position) is provided.

4.4. High-Pressure Freezing of Macromolecular Crystals

Macromolecular crystals typically contain between 30% and 90% of solvent (mainly water). Successful cryocooling of such crystals requires the use of cryoprotectants in order to suppress hexagonal ice formation and to convert the water to amorphous ice (vitrification). Finding optimal cryoconditions can be very time-consuming and the data quality is often degraded upon cryoprotection.
Hence, an alternative approach which allows sample vitrification without any cryoprotectants has been developed [23]. This method allows crycooling of macromolecular crystals at 210 MPa and 77 K directly in their aqueous crystallization solution. Our high-pressure freezing protocol was successfully applied to several types of macromolecular crystals including large unit cell systems, such as photosystem II and Bovine Enterovirus II, which represent very challenging targets for cryoprotection [24].

5. Acknowledgements

We thank our funding partners, the Max Planck Society, the Helmholtz Association (research field 'Health') and the University of Luebeck for financial support. We thank our users for their experimental feedback which helps us to continuously improve our beamline. Katja Fälber, Kathrin Schulte and Oliver Daumke (Max Delbrück Center for Molecular Medicine, Berlin) are gratefully acknowledged for contributing Figure 6 to this paper.

6. References

1) Franz, H., Leupold, O., Röhlsberger, R., Roth, S. V., Seeck, O. H., Spengler, J., Strempfer, J., Tischer, M., Viefhaus, J., Weckert, E. & Wroblewski, T. (2006). *Synchrotron Radiation News*, **19**, 25–29.

2) Balewski, K., Brefeld, W., Decking, W., Li, Y., Sahoo, G. K. & Wanzenberg, R. (2004). *Proceedings*

of EPAC, Lucerne, Switzerland, 2302–2304.

3) https://door.desy.de/door/index.php

4) http://photon-science.desy.de/users_area/users_guide/index_eng.html

5) http://www.biostruct-x.eu/content/apply-funding

6) http://photon-science.desy.de/facilities/petra_iii/beamlines/p11_bio_imaging_and_diffraction

7) http://www.embl-hamburg.de/services/mx/P13

8) http://www.embl-hamburg.de/services/mx/P14

9) Meents, A., Reime, B., Stuebe, N., Fischer, P., Warmer, M., Goeries, D., Roever, J., Meyer, J., Fischer, J., Burkhardt, A., Vartiainen, I., Karvinen, P. & David, C. (2013). *SPIE Optical Engineering + Applications, Proceedings of SPIE 8851*, San Diego, United States, p. 88510K.

10) Vartiainen, I., Warmer, M., Goeries, D., Herker, E., Reimer, R., David, C. & Meents, A. (2014). *J. Synchrotron Rad.*, **21**, 790–794.

11) Stachnik, K., Mohacsi, I., Vartiainen. I., Stuebe, N., Meyer, J., Warmer, M., David, C. & Meents, A. (2015). *Appl. Phys. Lett.* **107**, 011105.

12) http://www.suna-precision.com/

13) Kabsch, W. (2010). *Acta Cryst. D***66**, 125–132.

14) Leslie, A. G. W. (2006). *Acta Cryst. D***62**, 48–57.

15) Sheldrick, G. M. (2008). *Acta Cryst. A***64**, 112–122.

16) Adams, P. D., Afonine, P. V., Bunkóczi, G., Chen, V. B., Davis, I. W., Echols, N., Headd, J. J., Hung, L.-W., Kapral, G. J., Grosse-Kunstleve, R. W., McCoy, A. J., Moriarty, N. W., Oeffner, R., Read, R. J., Richardson, D. C., Richardson, J. S., Terwilliger, T. C. & Zwart, P. H. (2010). *Acta Cryst. D***66**, 213–221.

17) Winn, M. D., Ballard, C. C., Cowtan, K. D., Dodson, E. J., Emsley, P., Evans, P. R., Keegan, R. M., Krissinel, E., B., Leslie, A. G. W., McCoy, A., McNicholas, S. J., Murshudov, G. N., Pannu, N. S., Potterton, E. A., Powell, H. R., Read, R. J., Vagin, A. & Wilson, K. S. (2011). *Acta. Cryst. D***67**, 235–242.

18) Emsley, P., Lohkamp, B., Scott, W. G. & Cowtan, K. (2010). *Acta Cryst. D***66**, 486–501.

19) Dolomanov, O. V., Bourhis, L. J., Gildea, R. J., Howard, J. A. K. & Puschmann, H. (2009). *J. Appl. Cryst.* **42**, 339–341.

20) Roedig, P., Vartiainen, I., Duman, R., Panneerselvam, S., Stuebe, N., Lorbeer, O., Warmer, M., Sutton, G., Stuart, D. I., Weckert, E., David, C., Wagner, A. & Meents, A. (2015). *Scientific Reports*, **5**,

10451.

21) Hellmich, J., Bommer, M., Burkhardt, A., Ibrahim, M., Kern, J., Meents, A., Müh, F., Dobbek, H. & Zouni, A. (2014). *Structure*, **22**, 1607–1615.

22) Stellato, F., Oberthür, D., Liang, M., Bean, R., Gati, C., Yefanov, O., Barty, A., Burkhardt, A., Fischer, P., Gallia, L., Kirian, R. A., Meyer, J., Panneerselvam, S., Yoona, C. H., Chervinskii, F., Speller, E., White, T. A., Betzel, C., Meents, A. & Chapman, H. N. (2014). *IUCrJ*, **1**, 204–212.

23) Burkhardt, A., Warmer, M., Panneerselvam, S., Wagner, A., Zouni, A., Glöckner, C., Reimer, R., Hohenberg, H. & Meents, A. (2012). *Acta Cryst. F***68**, 495–500.

24) Burkhardt, A., Wagner, A., Warmer, M., Reimer, R., Hohenberg, H., Ren, J., Fry, E. E., Stuart, D. I. & Meents, A. (2013). *Acta Cryst. D***69**, 308–312.

TABLES & FIGURES

Table 1: Characteristics of the three MX beamlines at PETRA III.

Beamline	**P11**	**P13**[#]	**P14**[#]
General parameters and infrastructure			
Energy range	5.5 - 30 keV	4.5 - 17.5 keV	6 - 20 keV
Beam size (v × h)	4 × 9 μm^2 - 300 × 300 μm^2 with 2 × 10^{13} ph/s at 12 keV 1 × 1 μm^2 with > 2 × 10^{11} ph/s	Focused beam: 20 × 30 μm^2 with 10^{13} ph/s at 12 keV Defocused beam: 70 × 150 μm^2	5 × 5 μm^2 with 5 × 10^{12} ph/s at 12 keV (focused) to 300 μm with 10^{12} ph/s (circular aperture, unfocused beam)
Beam divergence	8 × 15 μrad rms (v × h)	< 0.15 mrad	< 0.3 mrad
Diffractometer	Single axis goniostat (horizontal spindle)	MD2 (horizontal spindle) with mini-kappa goniostat	MD3 (vertical spindle) with mini-kappa goniostat
Detector	Pilatus 6M-F (25 Hz)	Pilatus 6M-F (25 Hz)	Pilatus 6M-F (25 Hz)
Fluorescence detector	Vortex EM	ROENTEC X-FLASH	AMPTEK silicon drift detector
Sample preparation	S2 lab	S1 lab with heavy atom derivatisation unit	S1 lab with heavy atom derivatisation unit
Sample exchange			
Mounting mode	Automatically by Stäubli robot with in-house-designed gripper	Automatically by MARVIN robot	Manually
Supported puck format	Uni-pucks	SPINE pucks	-
Storage Dewar capacity	368 samples	150 samples	-
Cycle time between two crystals	20 s	< 1 min	-
Beamline control software			
User Interface	In-house-designed, Python-based GUI	mxCuBE v2 (ESRF)	mxCuBE v2 (ESRF)
Additional experiments	- Serial crystallography - 2D/3D scans (grid scan with and without rotation)	- Three-click centering Continuous 4D-scans between two centering points (helical)	- Three-click centering - Continuous 4D-scans between two centering points (helical) - In situ data collection from crystal plates

[#] Information on beamlines P13 and P14 were taken from the EMBL webpages [7, 8].

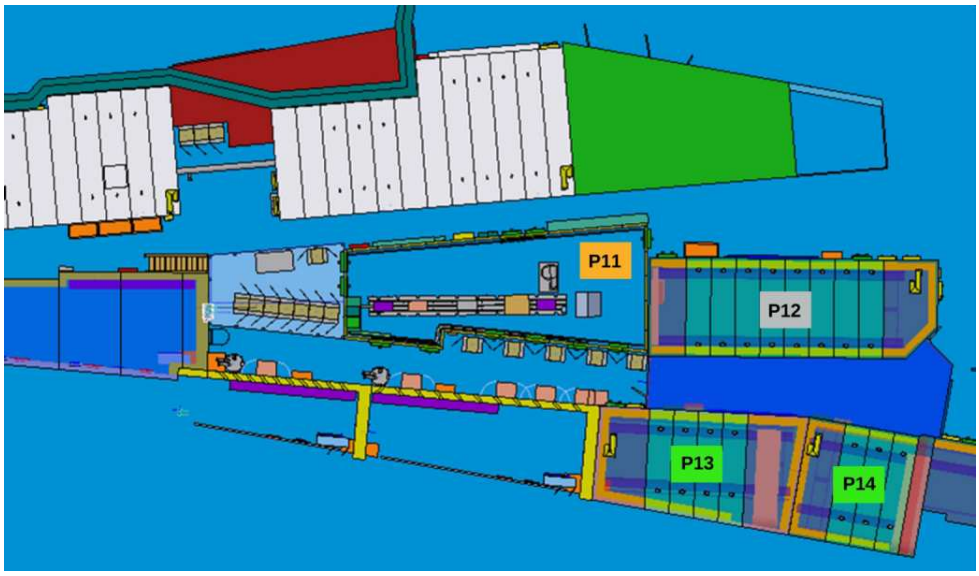

Figure 1: Floor layout of MX beamlines at PETRA III: P11 (orange), P13 and P14 (green). EMBL beamline P12 (grey) is dedicated to small angle scattering experiments on biological samples (BioSAXS) and is not described in this paper.

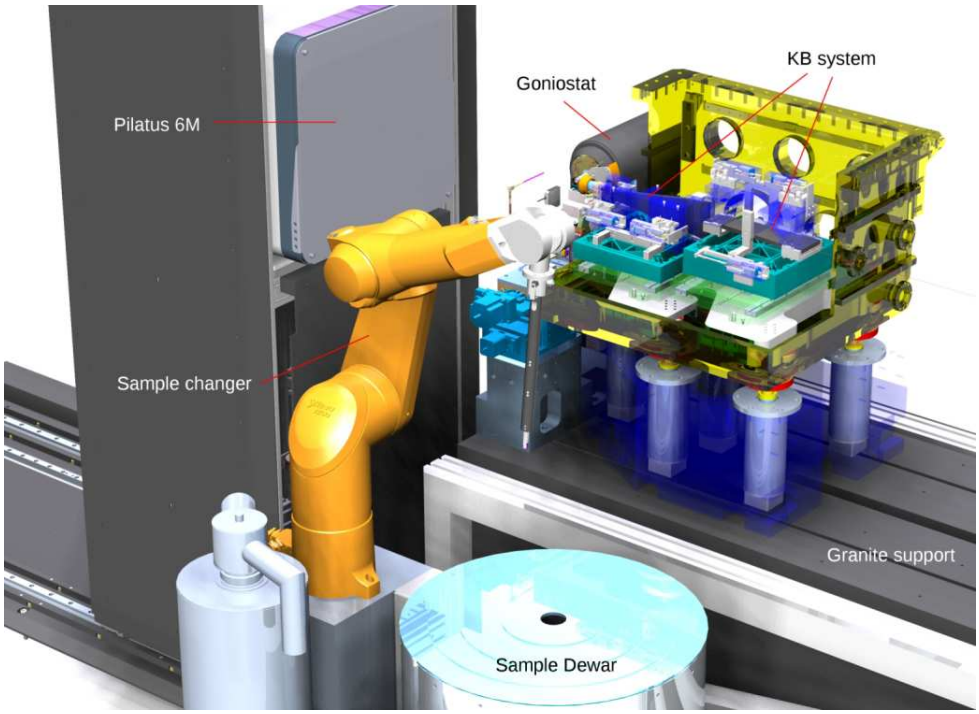

Figure 2: Overview of the crystallography endstation at beamline P11.

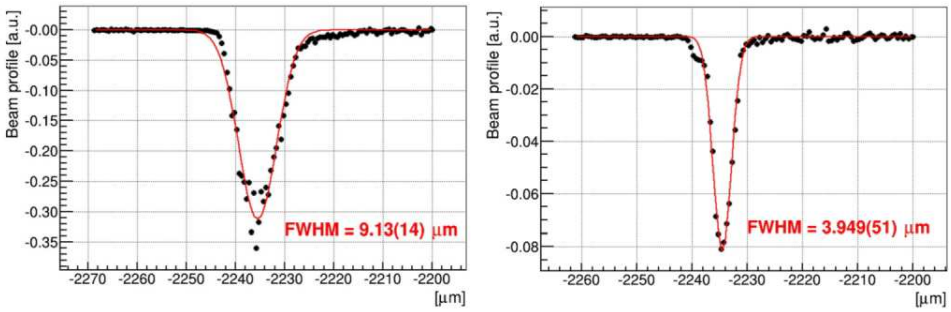

Figure 3: Horizontal beam profiles (dotted lines) of the P11 microbeam measured via knife-edge scans at 8 keV. The Gaussian fit to the experimental data is plotted as red solid line. Left panel: slits at secondary source fully open with a photon flux of 2×10^{13} ph/s (horizontal beam size: 9 µm); right panel: secondary source sliced down to 100×100 µm^2 with a photon flux of ~ 6×10^{12} ph/s (horizontal beam size: 4 µm). The corresponding vertical beam size was 4 µm for both scenarios.

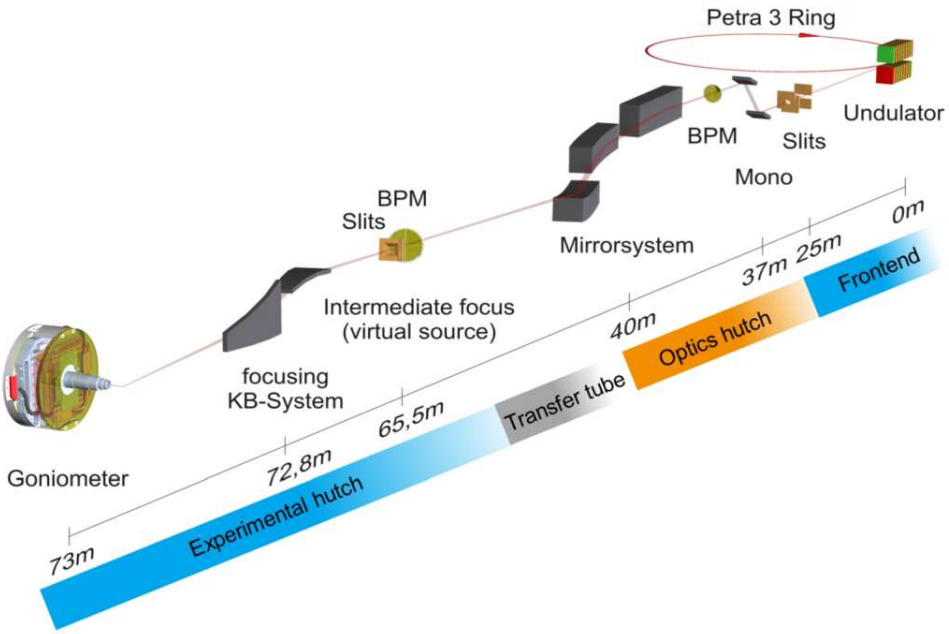

Figure 4: P11 beamline layout. The basis of the design is the generation of a secondary source at 65.5 m using the first three KB mirrors located in the optics hutch. With the second KB mirror system at 72.8 m in the experimental hutch, the X-ray beam can be focused into a spot of 4×9 µm^2 which allows for structural investigations of microcrystals.

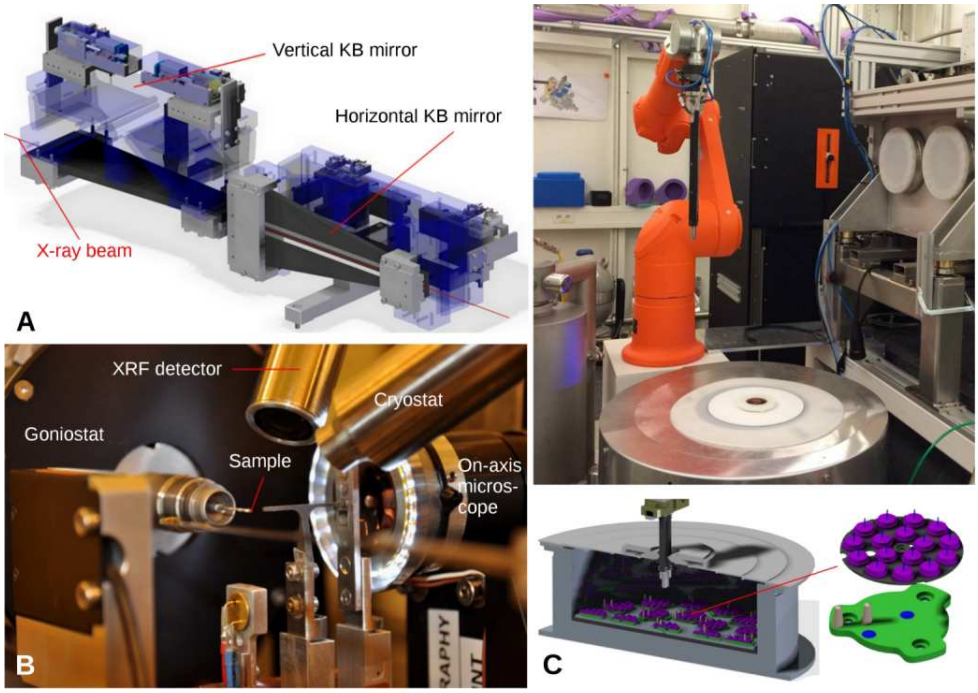

Figure 5: Key features of the P11 crystallography endstation. A: A second KB mirror system for microbeam capability; B: Single axis goniostat with piezo-driven centering stage for accurate sample positioning, on-axis microscope, apertures, collimator, flux diode and scintillator screen, XRF detector and cryojet nozzle; C: Automatic sample changer with large storage Dewar for high-throughput crystallography.

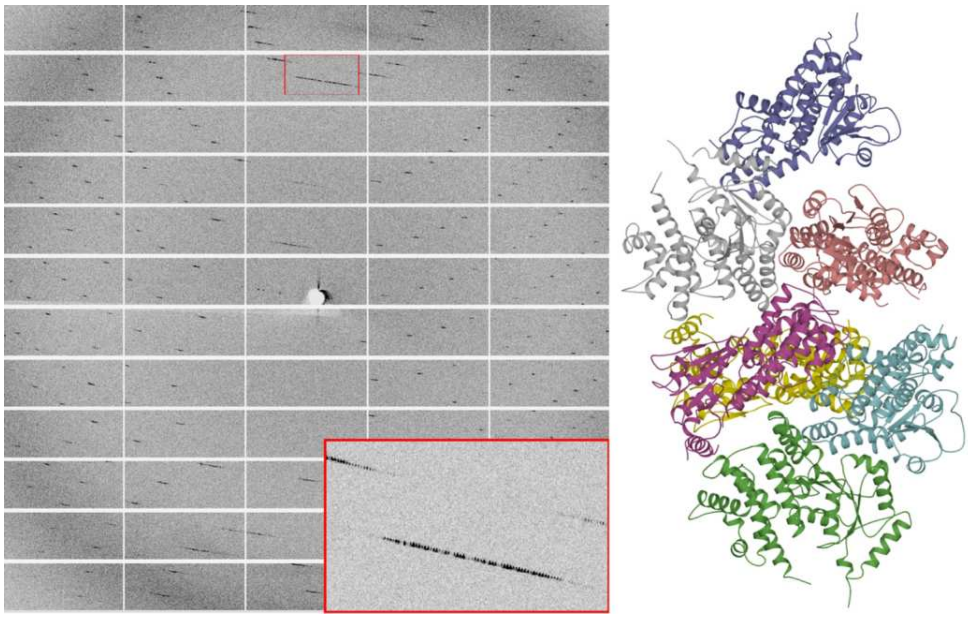

Figure 6: A diffraction image (left) and the refined structure (right) of a protein with a 1300 Å cell axis solved from data collected at beamline P11 are shown (Images were kindly provided by K. Fälber, K. Schulte and O. Daumke, Max Delbrück Center for Molecular Medicine, Berlin).

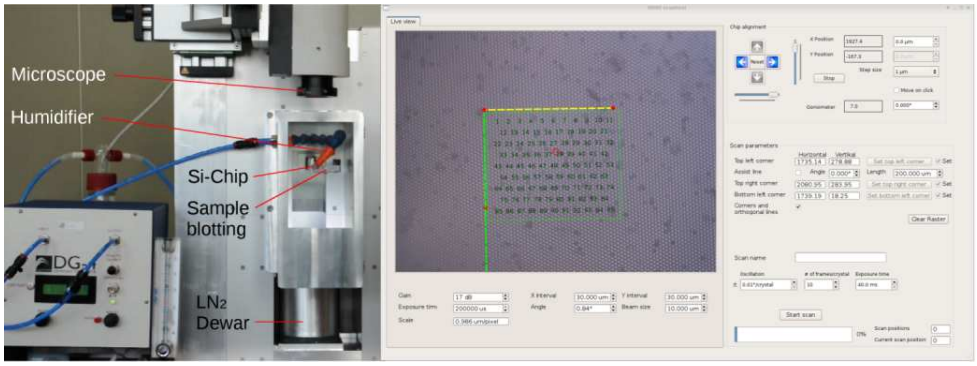

Figure 7: P11 infrastructure for serial crystallography experiments on microchips. The plunge-freezer for automatic chip-freezing (left) and a graphical user interface for automatic chip-scanning (right) are depicted. The grid (in green) defines the area to be scanned. Measurements can be performed with (3D) and without (2D) ϕ rotation at each position.